FEBS Letters

FEBS PRESS science publishing by scientists

COMMUNICATION

Improved recombinant expression and purification of functional plant Rubisco

Robert H. Wilson[1], Gabriel Thieulin-Pardo[1], Franz-Ulrich Hartl[2] and Manajit Hayer-Hartl[1]

1 Chaperonin-assisted Protein Folding Group, Max Planck Institute of Biochemistry, Martinsried, Germany
2 Cellular Biochemistry Group, Max Planck Institute of Biochemistry, Martinsried, Germany

Correspondence
M. Hayer-Hartl, Chaperonin-assisted Protein Folding Group, Max Planck Institute of Biochemistry, 82152 Martinsried, Germany
Tel: +49 89 8578 2204
E-mail: mhartl@biochem.mpg.de

Robert H. Wilson and Gabriel Thieulin-Pardo contributed equally to this article

(Received 8 February 2019, revised 24 February 2019, accepted 25 February 2019, available online 14 March 2019)

doi:10.1002/1873-3468.13352

Edited by Ulf-Ingo Flügge

Improving the performance of the key photosynthetic enzyme Ribulose-1,5-bisphosphate carboxylase/oxygenase (Rubisco) by protein engineering is a critical strategy for increasing crop yields. The extensive chaperone requirement of plant Rubisco for folding and assembly has long been an impediment to this goal. Production of plant Rubisco in *Escherichia coli* requires the coexpression of the chloroplast chaperonin and four assembly factors. Here, we demonstrate that simultaneous expression of Rubisco and chaperones from a T7 promotor produces high levels of functional enzyme. Expressing the small subunit of Rubisco with a C-terminal hexahistidine-tag further improved assembly, resulting in a ~ 12-fold higher yield than the previously published procedure. The expression system described here provides a platform for the efficient production and engineering of plant Rubisco.

Keywords: assembly; folding; molecular chaperones; protein expression; Rubisco; Rubisco activase

Ribulose-1,5-bisphosphate carboxylase/oxygenase (Rubisco), the key enzyme of the Calvin-Benson-Bassham cycle of photosynthesis, is responsible for the entry of atmospheric carbon dioxide (CO_2) into the biosphere by catalyzing the carboxylation of its five carbon sugar substrate ribulose-1,5-bisphosphate (RuBP). Plant Rubisco has a low catalytic rate (~ 2–5 $CO_2 \cdot s^{-1}$ per active site) and thus chloroplasts produce vast amounts of Rubisco, making up to 50% of the total leaf protein and reaching concentrations exceeding 200 $mg \cdot mL^{-1}$ [1–3]. Moreover, the specificity of Rubisco for CO_2 versus O_2 is limited, resulting in energetically wasteful oxygenation of RuBP, a process known as photorespiration [4]. Rubisco is a hexadecameric complex of ~ 530 kDa consisting of eight large (RbcL, ~ 53 kDa) and eight small (RbcS, 13 kDa) subunits. The RbcL subunit requires the chloroplast chaperonin (Cpn60) and its cofactors (Cpn20/Cpn10) for folding [2], but remains unstable and aggregation-prone prior to assembly with RbcS [5] (Fig. 1). As shown recently, assembly of the Rubisco holoenzyme ($RbcL_8S_8$) from *Arabidopsis thaliana* upon recombinant expression in *Escherichia coli* requires four auxiliary factors [5] (Fig. 1): Rubisco accumulation factor 1 (Raf1) [6,7]; Rubisco accumulation factor 2 (Raf2) [8–10]; Bundle sheath defective-2 (BSD2) [5,11]; and RbcX [12–15].

Modifications to plant Rubisco or heterologous expression of alternative isoforms is central to improving photosynthesis [16,17]. Reduction of

Abbreviations
Amp, ampicillin; BSD2, bundle sheath defective protein 2; Cam, chloramphenicol; Cpn, chloroplast chaperonin; ECM, enzyme-CO_2-magnesium; EI, enzyme inhibited; GAPDH, glyceraldehyde-3-phosphate dehydrogenase; GPDH, glycerol 3-phosphate dehydrogenase; Kan, kanamycin; NADH, nicotinamide adenine dinucleotide (reduced form); PGK, phosphoglycerate kinase; Raf, Rubisco accumulation factor; RbcL, Rubisco large subunit; RbcS, Rubisco small subunit; Rca, Rubisco activase; RuBP, ribulose-1, 5-biphosphate; SEC, size-exclusion chromatography; Spec, spectinomycin; TIM, triose phosphate isomerase.

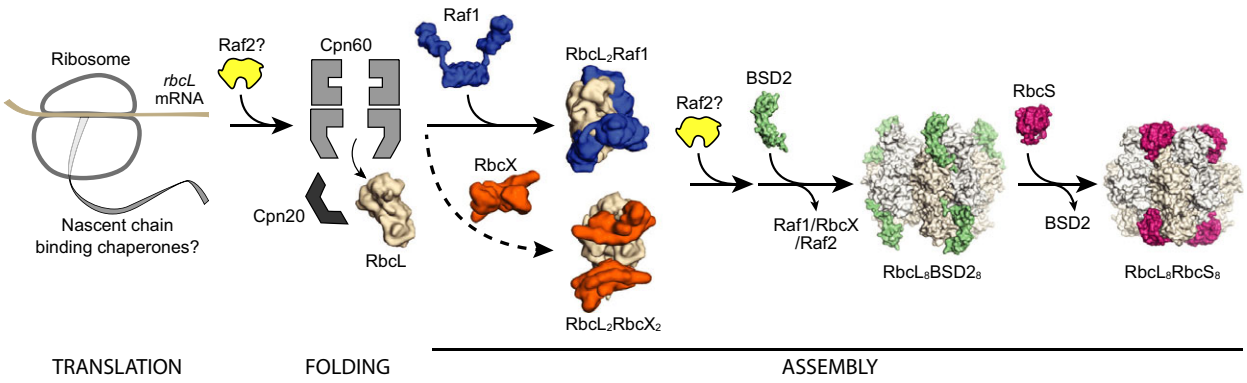

Fig. 1. Model of chaperone-assisted folding and assembly of plant Rubisco. Upon folding of newly synthesized RbcL subunits by the Cpn60αβ/Cpn20 chaperonin system, RbcL assembly to RbcL dimers and higher oligomers is mediated by Raf1 and RbcX acting in cooperation or in parallel. Binding of BSD2 causes the displacement of these factors and stabilizes $RbcL_8$ cores in a state competent for association with RbcS. RbcS binding causes displacement of BSD2, forming the functional holoenzyme. Raf2 is essential for Rubisco biogenesis [5]; however, its function is as yet unknown. Raf2 may act either downstream or upstream of the chaperonin system. Figure reproduced from Ref. [5].

Rubisco oxygenation activity can offer a large improvement to photosynthetic output [18] and improved carboxylation rates are predicted to provide similar enhancements [19]. Mutagenesis and engineering of Rubisco in plants is time-consuming and labor-intensive, with deleterious mutations resulting in crippled plants which can only grow in tissue culture [20–22]. Green algae, capable of heterotrophic growth, provide an alternative host for the analysis of plant Rubisco mutants. However, the incompatibility of assembly chaperones and low transformation efficiency limit the usefulness of this approach for high throughput screening in directed evolution [16]. Recombinant expression in a bacterial host would therefore greatly facilitate efforts at engineering plant Rubisco.

Functional bacterial expression of *A. thaliana* Rubisco was recently achieved using a sequential expression strategy where the chloroplast chaperonin and the four specific assembly chaperones were pre-expressed, followed by Rubisco induction [5]. This approach was designed to avoid overburdening the biosynthetic machinery. However, the yield of functional Rubisco was moderate. In this study, we present a simplified, highly efficient strategy to express and purify functional *A. thaliana* Rubisco from *E. coli*. The novel aspects of this strategy are the following: (a) Expression of Rubisco and all chaperones is simultaneously induced from isopropyl β-D-1-thiogalactopyranoside (IPTG) regulated plasmids. (b) RbcS is expressed with a C-terminal hexahistidine-tag which further improves assembly efficiency and facilitates purification of the holoenzyme.

Materials and methods

Plasmid construction

pET28-*At*RbcLS

The *rbcLS* operon was amplified from the vector pBAD33-*At*RbcLS [5] using the primers 5GibAtL and 3GibAtS. The backbone of the pET28b vector was amplified from the commercially available expression vector pET28b using the primers pET28bopenFor and pET28bopenRev (Table S1). The *rbcLS* and pET28b fragments were ligated using NEB Gibson Assembly® master mix (NEB), as per manufacturer's instructions, to generate the plasmid pET28-*At*RbcLS.

*At*RbcLS^{His6}

To introduce a C-terminal hexahistidine-tag (His6-tag) to *rbcS3* and create the plasmid pET28-*At*RbcLS^{His6}, the stop codon (TAA) at the end of the *rbcS3* coding sequence was replaced by an alanine codon (GCA) by site-directed mutagenesis (QuikChange site-directed mutagenesis kit; Agilent Technologies, Santa Clara, CA, USA) using the *rbcS3-his-fwd* and *rbcS3-his-rev* primers (Table S1), effectively fusing the coding sequence of *rbcS3* to the His6-tag of the pET28b vector, resulting in the insertion of the amino-acid sequence ALEHHHHHH at the C terminus of the RbcS protein.

pET28-Ub-*At*Rcaβ

The *A. thaliana* Rubisco activase (β isoform) (*At*Rcaβ) was cloned into the pHUE plasmid, which contains a N-terminal, cleavable fusion with His6-ubiquitin [23]. The His6-

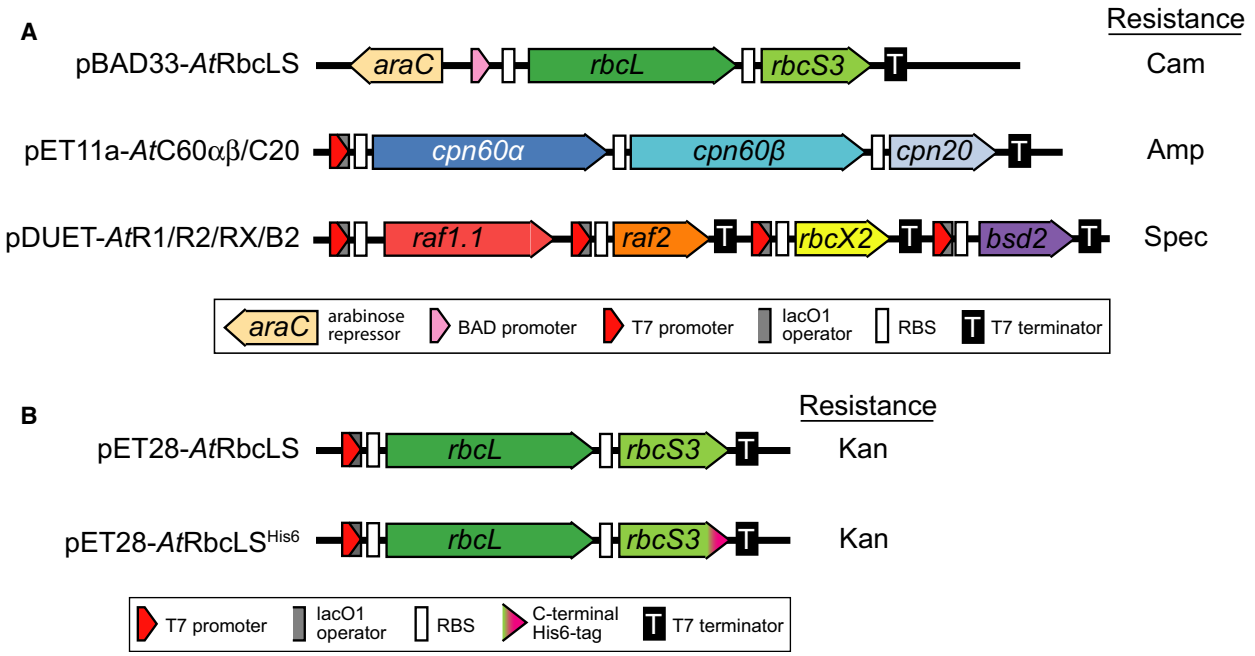

Fig. 2. (A) Operon organization of plasmids used in the sequential expression of auxiliary factors and Rubisco from *Arabidopsis thaliana* by induction with IPTG and arabinose [5]. Plasmid pBAD33-*At*RbcLS for the expression of *A. thaliana* RbcL and RbcS; plasmid pET11a-*At*C60αβ/C20 expressing the chloroplast chaperonin subunits Cpn60α, Cpn60β, and the chaperonin cofactor Cpn20; plasmid pDUET-*At*R1/R2/RX/B2 expressing the Rubisco assembly chaperones Raf1.2, Raf2, RbcX and BSD2. Cam, chloramphenicol; Amp, ampicillin; Spec, spectinomycin; RBS, ribosome-binding site. (B) Plasmids pET28-*At*RbcLS and pET28-*At*RbcLS^{His6} for the simultaneous expression by IPTG induction of *A. thaliana* RbcL/RbcS (without or with a C-terminal His6-tag on RbcS, respectively) and plasmids pET11a-*At*C60αβ/C20 and pDUET-*At*R1/R2/RX/B2 (Fig. 2A). Kan, kanamycin.

ubiquitin *At*Rcaβ was cloned into a pET28b vector between NcoI and XhoI restriction sites to generate the pET28-Ub-*At*Rcaβ plasmid.

Protein expression

Escherichia coli were grown using Luria-Bertani (LB) broth or LB agar containing the following antibiotic concentrations when required: 100 $\mu g \cdot mL^{-1}$ ampicillin (Amp), 32 $\mu g \cdot mL^{-1}$ chloramphenicol (Cam), 100 $\mu g \cdot mL^{-1}$ spectinomycin (Spec), and/or 30 $\mu g \cdot mL^{-1}$ kanamycin (Kan). The *E. coli* strain BL21 Star™ (DE3) (Thermo Fisher Scientific Inc., Waltham, MA, USA), designed to improve mRNA stability [24], was used for new bacterial cell line constructions. This strategy was used to improve Rubisco yield consistency between experiments. As shown previously, each open reading frame (ORF) requires its own ribosome-binding site for successful plant Rubisco assembly in *E. coli* [5] (Fig. 2). Plasmid pET11a-*At*C60αβ/C20 was transformed into electrocompetent BL21 Star™ (DE3) cells which were recovered and plated to LB agar containing Amp prior to growth at 37 °C. These cells were then prepared as electrocompetent and transformed with plasmid pDUET-*At*R1/R2/RX/B2 and recovered on LB agar containing Amp and Spec. Again electrocompetent cells were prepared and transformed with either plasmid pET28b or pET28-*At*RbcLS or pET28-*At*RbcLS^{His6} and recovered on LB agar containing Amp, Spec, and Kan. The strain expressing *A. thaliana* Rubisco under arabinose induction was generated by transforming the electrocompetent cells containing plasmids pET11a-*At*C60αβ/C20 and pDUET-*At*R1/R2/RX/B2 with plasmid pBAD33-*At*RbcLS [5], and was propagated on LB agar containing Amp, Spec, and Cam.

Bacterial cultures of each strain were prepared by picking colonies from agar plates and transferring them to 5 mL liquid LB media containing the required antibiotics. These starter cultures were incubated overnight at 37 °C and 220 r.p.m. shaking. The following day 500 µL of starter culture was used to inoculate 50 mL of the same media and incubated at 37 °C and 220 r.p.m. until the culture reached an OD_{600} of ~ 0.7. For simultaneous expression of chaperonin, auxiliary factors and Rubisco, cultures of *E. coli* harboring pET28b-based Rubisco and chaperone expression plasmids were first equilibrated to 23 °C and then IPTG added to a final concentration of 0.5 mM and incubated at 23 °C at 150 r.p.m. for ~ 16 h. The following day, 40 mL of the culture was pelleted at 4000 ***g*** at 4 °C in 50 mL falcon tubes. The resulting pellet was processed immediately or flash-frozen in liquid nitrogen and stored at −20 °C. To express the chaperone factors and Rubisco

sequentially, *E. coli* cells harboring the plasmid pBAD33-*At*RbcLS and the pET28b-based chaperone expression plasmids were first induced with IPTG for 4 h, followed by centrifugation at 4000 ***g*** at 4 °C in 50 mL falcon tubes. The supernatant was discarded and the cell pellet resuspended in fresh 50 mL LB media containing antibiotics and 0.4% (w/v) L-arabinose and incubated at 23 °C, 150 r.p.m., for ~ 16 h for expression of Rubisco [5]. About 40 mL of the culture was pelleted as described above and either processed immediately or flash-frozen in liquid nitrogen and stored at −20 °C.

The β isoform of Rubisco activase from *A. thaliana* (*At*Rcaβ) was expressed in *E. coli* BL21 cells transformed with pET28-Ub-*At*Rcaβ and plasmid p*Ec*EL/ES for overexpression of GroEL/ES chaperonin [5] in presence of 0.3 mM IPTG for 10 h.

Protein purification

Purification of Rubisco from *A. thaliana* leaves

Arabidopsis thaliana leaves (60 g) were ground in the presence of liquid nitrogen. The resulting fine powder was suspended in extraction buffer (30 mM Tris pH 7.9, 4 mM EDTA, 5 mM DTT, 1 mM PMSF, 10% glycerol), filtered and centrifuged (57 000 ***g***, 30 min, 4 °C, TI45 rotor; Beckman Coulter, Brea, CA, USA). The clarified lysate was loaded on a self-cast DEAE column equilibrated with buffer (30 mM Tris pH 7.9, 4 mM EDTA, 1 mM DTT), and the bound proteins were eluted by a salt gradient of NaCl (0–0.35 M). Fractions containing Rubisco were pooled and loaded on a HiPrep 26/60 Sephacryl S-300 HR size-exclusion chromatography (SEC) column (GE Healthcare, Chicago, IL, USA) equilibrated with SEC buffer (30 mM Tris pH 7.9, 1 mM EDTA, 1 mM DTT, 150 mM NaCl). Fractions containing Rubisco were pooled and concentrated; glycerol was added to a final concentration of 10% and aliquots stored at −80 °C.

Purification of recombinant His-tagged Rubisco

Tagged Rubisco was purified from *E. coli* BL21 DE3(Star) cells transformed with plasmids pET11a-*At*C60αβ/C20, pDUET-*At*R1/R2/RX/B2, and pET28-*At*RbcLS^{His6} and expressed in 6 L LB media, as described above, in the presence of 0.3 mM IPTG for 10 h at 23 °C. The cell pellet was resuspended in extraction buffer (30 mM Tris pH 7.9, 150 mM NaCl, 10 mM imidazole, 0.5 g·L^{-1} lysozyme, 5 U·mL^{-1} benzonase, 5% glycerol), disrupted by sonication and centrifuged (70 000 ***g***, 30 min, 4 °C, TI45 rotor; Beckman Coulter). The clarified lysate was then loaded on a nickel-nitrilotriacetic acid (Ni-NTA) column (HisTrap 5 mL; GE Healthcare) equilibrated with NTA buffer (30 mM Tris pH 7.9, 150 mM NaCl, 10 mM imidazole, 5% glycerol), and bound proteins were eluted using a gradient of imidazole (10–300 mM). Fractions containing Rubisco were pooled and loaded on a HiPrep 26/60 Sephacryl S-300 HR column equilibrated with SEC buffer. Fractions containing Rubisco were then pooled, concentrated, and stored as above.

Purification of recombinant Rubisco activase

The β isoform of Rubisco activase from *A. thaliana* (*At*Rcaβ) was purified from *E. coli* BL21 DE3(Star) cells transformed with plasmid pET28-Ub-*At*Rcaβ and plasmid p*Ec*EL/ES and expressed in LB medium. *E. coli* cells were resuspended in extraction buffer (30 mM Tris pH 7.9, 150 mM NaCl, 10 mM imidazole, 0.5 g·L^{-1} lysozyme, 5 U·mL^{-1} Benzonase, 5% glycerol), disrupted by sonication and centrifuged (70 000 ***g***, 30 min, 4 °C, TI45 rotor; Beckman Coulter). The clarified lysate was then loaded on a Ni-NTA column (HisTrap 5 mL; GE Healthcare) equilibrated with NTA buffer, and bound proteins were eluted using an imidazole gradient of 10–300 mM. Fractions containing Rubisco activase were pooled, treated by the deubiquitinase enzyme Usp2 (0.5 mg) [23] in presence of 0.05% β-mercaptoethanol for 3 h to remove the ubiquitin tag and loaded on a HiPrep 26/60 Sephacryl S-300 HR column equilibrated with SEC buffer. Fractions containing AtRcaβ were pooled, concentrated, and stored as above.

All purified protein were quantified by absorbance at 280 nm using a NanoDrop 1000 spectrophotometer (Thermo Fisher Scientific) using extinction coefficients of 103 250 M^{-1}·cm^{-1} for *At*RbcLS (MW 73 153.2 Da) and *At*RbcLS^{His6} (MW 74 289.4 Da), and 36 270 M^{-1}·cm^{-1} for *At*Rcaβ (43 308 Da).

Cell fractionation and immunoblotting

Bacterial pellets were resuspended in Rubisco extraction buffer consisting of 50 mM Tris-HCl pH 8.0, 10 mM $MgCl_2$, 1 mM EDTA, 30 mM $NaHCO_3$, Complete™ protease inhibitor cocktail (Roche, Basel, Switzerland), 7.5 U·mL^{-1} *Serratia marcescens* nuclease (MPIB core facility), 1 mg·mL^{-1} lysozyme) and incubated on ice for 30 min. Cells were lysed by sonication using a Sonifier 250 (Branson Ultrasonics, Danbury, CT, USA) over a 5-min duration with intensity setting 3 at 0.3 s sonic bursts. A sample of the resulting solution was taken as the 'total lysate' protein fraction and the soluble protein fraction was obtained by centrifugation at 16 000 ***g*** for 10 min at 4 °C. The protein amount in the soluble fraction was quantified by Bradford assay in UV flat bottom 96 well Microtitre® plates (Thermo Fisher Scientific). Soluble protein fraction was diluted 100-fold in deionized water and diluted in triplicate wells at a 10 : 140 µL ratio with deionized water. An equivalent volume of Coomassie plus™ protein assay reagent (Thermo Fisher Scientific) was added to each well and after 5 min absorption at 595 nm was measured using the Apollo 11 LB 913 microplate reader (Berthold Technologies, Bad Wildbad, Germany). Protein amount was determined relative to the BSA protein

standardized curve in each plate, containing 0–2.25 μg gradient of high-quality Pierce™ BSA (Thermo Fisher Scientific).

Soluble protein was diluted with 4× native-PAGE loading buffer (200 mM Tris-HCl, 0.4% bromophenol blue, 40% glycerol) and 20 μg of soluble protein lysate was loaded on Novex™ 4–12% Tris-Glycine Native-PAGE gradient mini gels (Thermo Fisher Scientific) followed by separation at 150 V for 90 min at 4 °C in 1× native-PAGE running buffer (25 mM Tris-HCl pH 8.3, 190 mM glycine). For SDS/PAGE analysis, soluble protein was diluted with 4× SDS/PAGE loading buffer [200 mM Tris-HCl pH 6.8, 0.4% bromophenol blue, 40% (v/v) glycerol, 8% (w/v) SDS] and 12 μg of soluble or total protein lysate was loaded on Novex™ 4–12% Bis-Tris NuPAGE gradient mini gels (Thermo Fisher scientific) followed by separation at 150 V for 90 min at 4 °C in 1× SDS/PAGE running buffer (50 mM MES pH 7.3, 50 mM Tris(hydroxymethyl)aminomethane, 0.1% (w/v) SDS, 1 mM EDTA).

Immunoblotting was performed using the semidry transfer method on in-house constructed transfer modules. Protein was transferred to a 0.45 μm Amersham™ Protran™ nitrocellulose blotting membrane (GE Healthcare) at 275 mA for 50 min. Membranes were blocked in 5% (w/v) skim milk powder in TBS buffer (50 mM Tris-HCl pH 7.5, 150 mM NaCl) for 1 h before probing with primary antibody for 45 min. Anti-Rubisco antibody (raised against *Nicotiana tabacum* Rubisco) was a kind gift from S. Whitney (Australian National University). Membranes were then washed thoroughly in TBS buffer before probing with anti-rabbit peroxidase conjugated IgG secondary antibody (Sigma-Aldricht, St. Louis. MO, USA) for 45 min in TBS buffer. Immunoblots were visualized using an ImageQuant LAS4000 mini (GE Healthcare) imager immediately after exposure to Immobilon® Classico western HRP substrate (Millipore, Burlington, MA, USA).

Rubisco carboxylation assay

Carboxylation assays were performed using purified Rubisco protein or soluble bacterial protein extract in 1.5 mL Eppendorf tubes. Each tube contained 108 μL of assay buffer (50 mM Tris-HCl pH 8.0, 10 mM MgCl, 1 mM EDTA, 30 mM $NaHCO_3$), 2 μL of ^{14}C labeled bicarbonate ([^{14}C]-$NaHCO_3$) and 20 μL of 5 mM D-ribulose-1,5-bisphosphate (RuBP; Sigma). The carboxylation assay at 25 °C was started by the addition of either 20 μL of soluble cell lysate or 20 μL of 62.5 nmol activated purified Rubisco, and stopped after 3 min by the addition of 50 μL of 50% (v/v) formic acid. Control reactions were in the absence of RuBP. Each assay set was accompanied by standard assays in quadruplicate. Standard assays were identical but contained 10-fold less RuBP (20 μL of 0.5 mM RuBP), were started with the addition of 1 mg of purified Rubisco from *A. thaliana* leaves, and were reacted for at least 30 min to completely convert the RuBP to product. Stopped reactions were dried in heat blocks at 98 °C until all solvent was removed. Reaction residues were dissolved in 500 μL of Milli-Q® H_2O and mixed with 750 μL of Rotiszint® eco plus LCS-Universalcocktail (Carl Roth, Karlsruhe, Germany) before measurement in an Aloka accuflex LSC-8000 scintillation counter (Hitachi, Chiyoda, Tokyo, Japan). Total fixed CO_2 can be determined per sample relative to the radioactivity of the standard assays which contained a known molar amount of RuBP. Rubisco in cell lysates was preactivated by the presence of $NaHCO_3$ in the extraction buffer (50 mM Tris-HCl pH 8.0, 10 mM $MgCl_2$, 1 mM EDTA, 30 mM $NaHCO_3$, Complete™ protease inhibitor cocktail (Roche), 7.5 $U \cdot mL^{-1}$ *S. marcescens* nuclease (MPIB core facility), 1 $mg \cdot mL^{-1}$ lysozyme).

Reactivation of Inhibited Rubisco

Inhibition of Rubisco was achieved by incubation of Rubisco in inactivation buffer (20 mM Tricine pH 7.9, 150 mM NaCl, 0.2 mM EDTA, N_2 sparged) and subsequent incubation with 2 mM RuBP to generate the RuBP-inhibited form (EI), or 20 mM $NaHCO_3$ and 20 mM $MgCl_2$ to generate the activated Rubisco (ECM).

Rubisco CO_2 fixation was measured through the oxidation of NADH by a coupled enzymatic assay modified from Kubien *et al.* [25] and Tsai *et al.* [26]. Reactions were performed using Rubisco at a concentration of 0.375 μM active sites, corresponding to 0.047 μM Rubisco holoenzyme, and Rubisco activase (when indicated) at a concentration of 0.67 μM hexamer. Reactions were initiated by the addition of Rubisco (and Rubisco activase) to the reaction buffer (100 mM Tricine pH 8.0, 10 mM $MgCl_2$, 10 mM $NaHCO_3$, 5 mM DTT, 2 mM RuBP, 0.5 mM NADH, 2 mM ATP, 5 U GAPDH, 5 U PGK, 5 U TIM, 5 U GPDH, 5 U creatine kinase).

Results

Improved Rubisco yields upon IPTG induction

The previous study achieving expression of functional *A. thaliana* Rubisco involved the generation of three plasmids for sequential expression of chaperones and Rubisco [5] (Fig. 2A): The plasmid pBAD33-*At*RbcLS for expression of RbcL and RbcS subunits of Rubisco under the control of the arabinose-regulated pBAD promoter (*araC* regulated); the plasmid pET11a-*At*C60αβ/C20 to express the chloroplast Cpn60 subunits α and β [2], and cofactor Cpn20 under the IPTG-inducible T7 promoter; plasmid pDUET-*At*R1/R2/RX/B2 for expression of Raf1, Raf2, RbcX, and BSD2, with each open reading frame (ORF) under control of the T7 promoter. Importantly, all ORFs are preceded by a ribosome-binding site (RBS) (Fig. 2A). Plasmids pET11a-*At*C60αβ/C20 and pDUET-*At*R1/

R2/RX/B2 were expressed for 3 h by induction with IPTG, followed by removal of IPTG and expression of Rubisco with arabinose for 18 h at 23 °C [5]. While this strategy was successful, the discontinuous expression of the chaperones probably limited the yield of Rubisco. Indeed, transfer of the *AtrbcLS* operon to the pET28b vector (Fig. 2B) and simultaneous expression with the two chaperone plasmids (10 h at 23 °C) greatly improved the production of assembled Rubisco detectable by native-PAGE, compared to sequential expression (Fig. 3A, lanes 1 and 3). Analysis of the carboxylation activity in equivalent amounts of *E. coli* lysate showed a ~ 6-fold increase in Rubisco activity (Fig. 3B, lanes 1 and 3).

In order to facilitate purification of the holoenzyme, we attached a hexahistidine-tag (His6-tag) to the C terminus of RbcS to generate the plasmid pET28-*At*RbcLS^{His6} (Fig. 2B). Interestingly, the expression of RbcS^{His6} doubled the yield of Rubisco holoenzyme and the carboxylation activity compared to the nontagged RbcS (Fig. 3A,B, lanes 3 and 4) resulting in a yield ~ 12-fold higher than with arabinose induction of RbcL and RbcS (Fig. 3B, lanes 1 and 4).

Analysis of total *E. coli* lysate by SDS/PAGE showed that much higher levels of total and soluble RbcL and RbcS are produced under the T7 promoter, compared to arabinose induction (Fig. 4A,B, lanes 1 and 3). This is consistent with the 6-fold higher yield of active Rubisco (Fig. 3B, lanes 1 and 3). Interestingly, the soluble RbcS was further increased when expressed with a His6-tag (Fig. 4A,B, lanes 3 and 4). Thus, improved solubility of RbcS^{His6} compared to the nontagged RbcS is responsible for the further ~ 2-fold increase in Rubisco production (Fig. 3B, lanes 3 and 4), resulting in a ~ 12-fold yield increase compared to the previously published procedure [5].

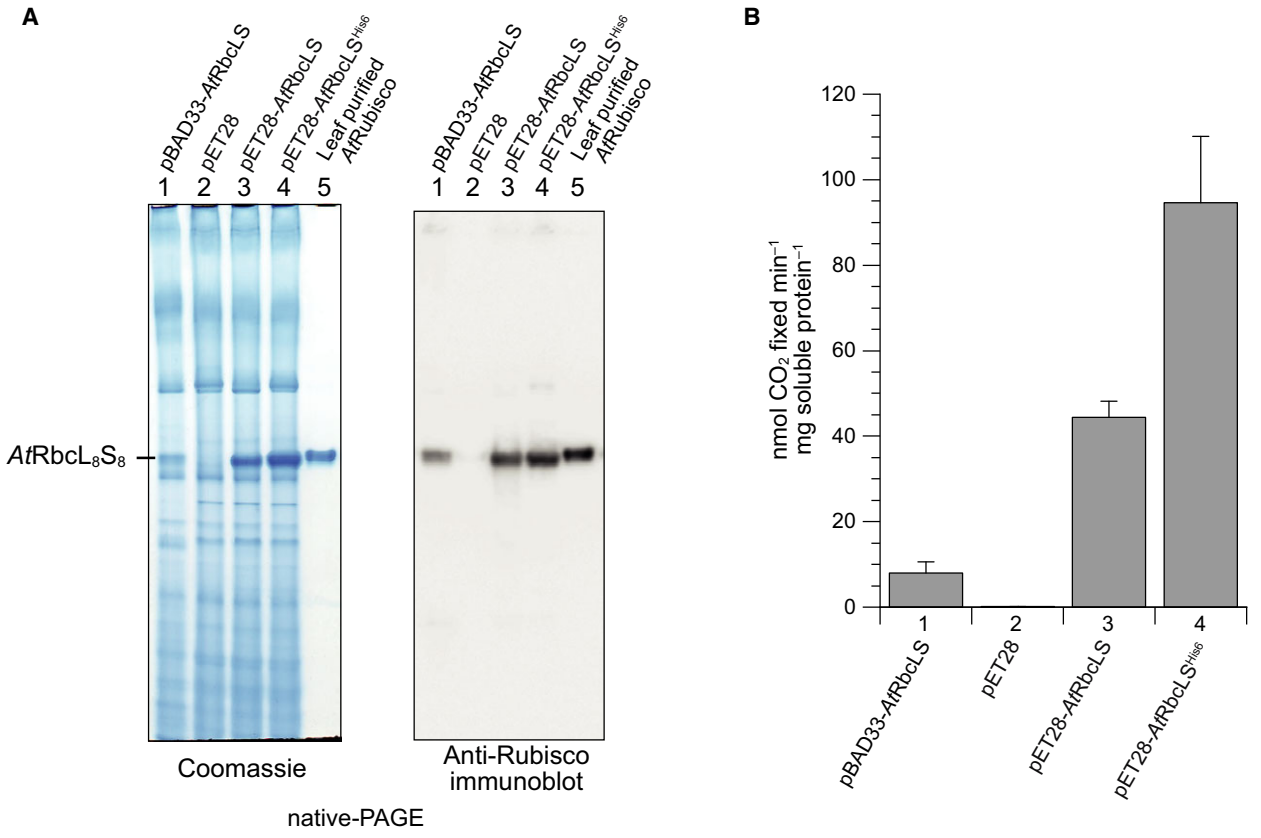

Fig. 3. Rubisco holoenzyme (*At*RbcL$_8$S$_8$) content in *Escherichia coli* cell extracts. (A) *Arabidopsis thaliana* chaperones and RbcL/RbcS were expressed either sequentially, as described previously [5] (lane 1) or simultaneously (lanes 3 and 4) using the RbcL/RbcS plasmids indicated, with pET28b (lane 2) as empty vector control. RbcS was expressed either without (lane 3) or with C-terminal His6-tag (lane 4). Rubisco purified from *A. thaliana* leaves was used as standard (0.8 μg, lane 5). Soluble extracts of *E. coli* cells containing 20 μg of total protein were analyzed by native-PAGE followed by Coomassie staining (left panel) or anti-Rubisco immunoblotting (right panel). The position of *At*RbcL$_8$S$_8$ holoenzyme is indicated. (B) Rubisco carboxylation activity in the cell lysates analyzed in (A). Activity is expressed as nmol CO_2 fixed per minute in 1 mL of cell extract with a total protein concentration of 1 mg·mL^{-1}. Error bars represent the SD of 8–18 measurements from $n = 4$ independent biological repeats.

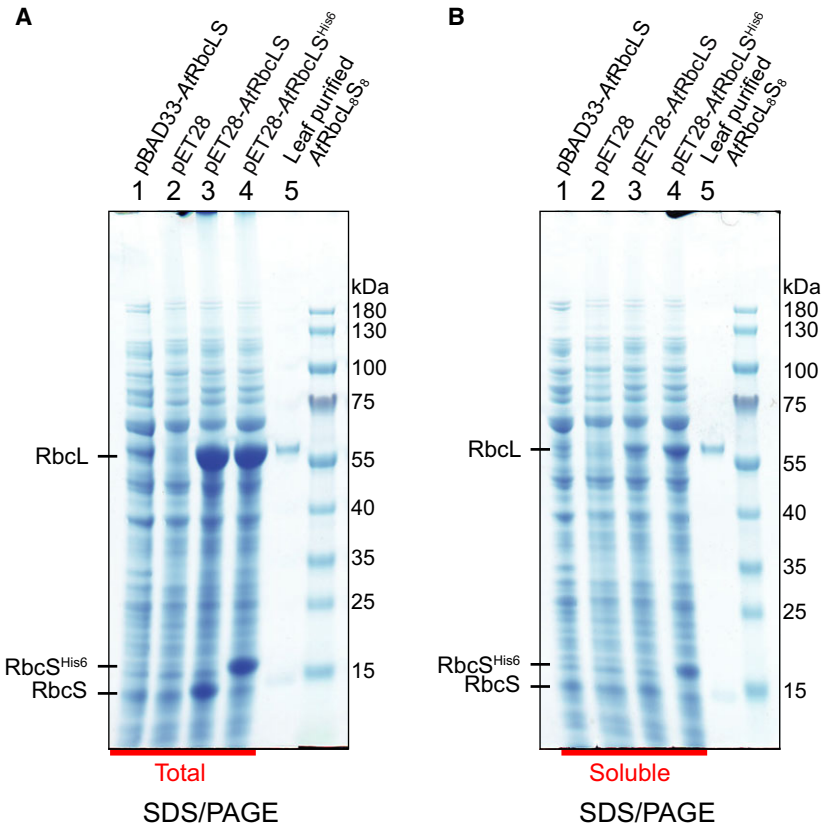

Fig. 4. *At*RbcL and *At*RbcS content in total (A) and soluble (B) *Escherichia coli* lysate. Total and soluble lysate fractions (10 μg of protein) from cells expressing auxiliary factors and RbcL/RbcS either sequentially (lanes 1) or simultaneously (lanes 3 and 4) from the indicated plasmids as in Fig. 3 were analyzed by SDS/PAGE and Coomassie staining. pET28b (lane 2) served as empty vector control and Rubisco purified from *Arabidopsis thaliana* leaves was used as standard (0.4 μg, lane 5). The positions of RbcL, RbcS and RbcS^{6His} are indicated. Note the increased amount of soluble RbcL and RbcS when RbcS is His6-tagged.

Purification and activity of His-tagged Rubisco

Using the improved expression system with pET28-*At*RbcLS^{His6}, we purified the recombinant *At*RbcL$_8$S$_8$^{His6} protein using a Ni-NTA affinity column (see Materials and methods) (Fig. 5A, lane 3 and Fig. S1). Free RbcS^{His6} was removed by size-exclusion chromatography (Fig. 5A, lane 4 and Fig. S2). We obtained 75 mg of purified recombinant *At*RbcL$_8$S$_8$^{His6} from a 6 L culture of *E. coli*. The purity of the recombinant protein was comparable to that of Rubisco purified from leaves based on SDS/PAGE and analysis by native-PAGE (Fig. 5B). The recombinant protein *At*RbcL$_8$S$_8$^{His6} showed a carboxylation activity similar to the enzyme purified from *A. thaliana* leaves (Fig. 5C), indicating that the tagged RbcS has no negative effect on Rubisco activity.

Inhibited recombinant Rubisco can be reactivated by Rubisco activase

Catalytic activity of Rubisco requires activation of the newly assembled protein by carboxylation at the active-site lysine by a nonsubstrate CO_2 molecule followed by binding of Mg^{2+}, a process called carbamylation [27]. Premature binding of the substrate, RuBP, to uncarbamylated Rubisco results in an inactive enzyme [28]. To activate the enzyme, the bound RuBP must be removed by Rubisco activase, an ATPase associated with various cellular activities (AAA+) protein, in an ATP-dependent reaction [19,29–31]. Although the C-terminal His6-tag on RbcS did not impede the assembly and the carboxylation activity of the recombinant Rubisco, we next investigated whether the His6-tag interferes with the recognition and subsequent reactivation of the inhibited enzyme by *A. thaliana* Rubisco activase β-isoform (*At*Rcaβ) [32–35]. The uncarbamylated *At*RbcL$_8$S$_8$^{His6}, like the leaf synthesized *At*RbcL$_8$S$_8$, could be inhibited by RuBP (EI), showing essentially no CO_2 fixation as a function of time (Fig. 6A,B). Both RuBP-inhibited Rubisco enzymes were efficiently reactivated by *At*Rcaβ in presence of ATP, reaching similar activities as the carbamylated enzymes (ECM) (Fig. 6A,B). These findings indicate that the C-terminal His6-tag on RbcS does not impede the recognition and remodeling of Rubisco by its cognate Rca.

Discussion

We have shown here that production of plant Rubisco in *E. coli* is best achieved using high induction and/or high copy number vectors for RbcL and RbcS

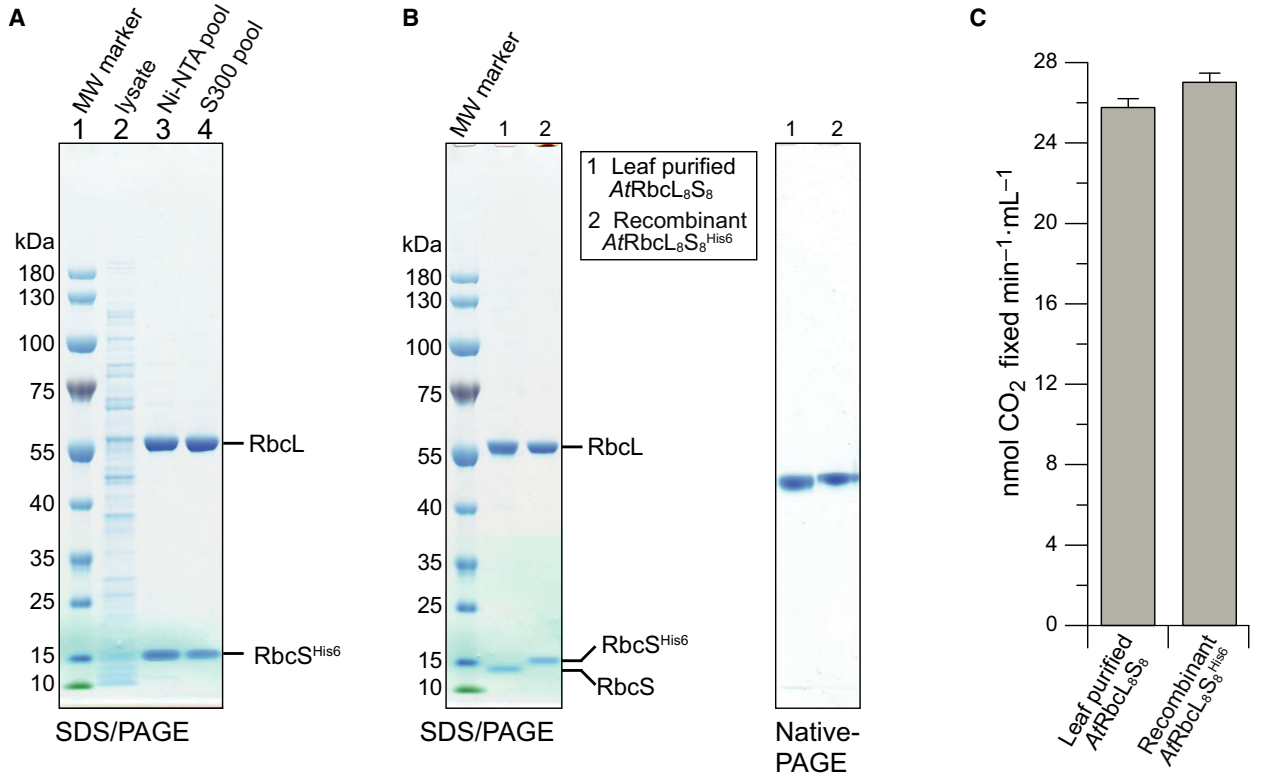

Fig. 5. Purification and characterization of recombinant *At*RbcL$_8$S$_8$ Rubisco. (A) Purification of *At*RbcL$_8$S$_8$^{His6}. Total cell lysate, the pooled fractions upon elution from Ni-NTA (Ni-NTA pool) and the pooled fractions upon size-exclusion chromatography (S300 pool) were analyzed by SDS/PAGE (2 μg protein for each sample) and Coomassie staining. The positions of RbcL and RbcS^{His6} are indicated. (B) SDS/PAGE comparing purified *At*RbcL$_8$S$_8$ from *Arabidopsis thaliana* leaves (lane 1) and recombinant *At*RbcL$_8$S$_8$^{His6} (lane 2) by SDS/PAGE (left panel) and native-PAGE (right panel). Two micrograms of protein was loaded. (C) Rubisco carboxylation activity of purified leaf *At*RbcL$_8$S$_8$ and recombinant *At*RbcL$_8$S$_8$^{His6}. Activity is expressed as nmol CO_2 fixed per minute in 1 mL reactions containing 0.0625 μM purified RbcL$_8$S$_8$. Error bars represent the SD of $n = 6$ independent measurements.

expression. Simultaneous rather than sequential expression of chaperones and Rubisco allows for efficient folding and assembly of the plant Rubisco. An important additional improvement in Rubisco yield was achieved by attaching a C-terminal hexahistidine-tag to RbcS. This resulted in stabilization of RbcS in a soluble state competent for assembly. In the previously published expression scheme, expression of RbcS was apparently limiting for Rubisco holoenzyme formation, which resulted in the accumulation of the penultimate assembly intermediate of RbcL with bound chaperone BSD2 (RbcL$_8$BSD2$_8$) [5]. Displacement of BSD2 by RbcS completes holoenzyme formation [5,36]. Apparently, the higher levels of RbcS achieved with the tagged protein increased the efficiency of this process, and avoided the accumulation of the BSD2 assembly intermediate observed with the sequential expression scheme [5]. The limited stability and hence solubility of unassembled RbcS above a concentration of ~ 2 mg·mL^{-1} [13] may suggest a specific chaperone requirement. Indeed, RbcS folds following import into chloroplasts in a reaction involving the organellar Hsp70 chaperone system [37,38]. Thus, additional overexpression of Hsp70 system in *E. coli* may further improve solubility. The C-terminal His6-tag on RbcS also facilitated the purification of recombinant Rubisco holoenzyme. Importantly, the tagged Rubisco was fully functional and the RuBP-inhibited enzyme was efficiently recognized by the AAA+ protein Rubisco activase.

The improved expression method as well as the facile and efficient purification protocol described here provides a versatile platform for studies involving functional and structural characterization of mutations of higher plant Rubisco. As the pET28 and pET11a plasmids (for expression of Rubisco and chaperonins, respectively) share the pBR322 origin of replication, the long-term coexistence of these plasmids may result

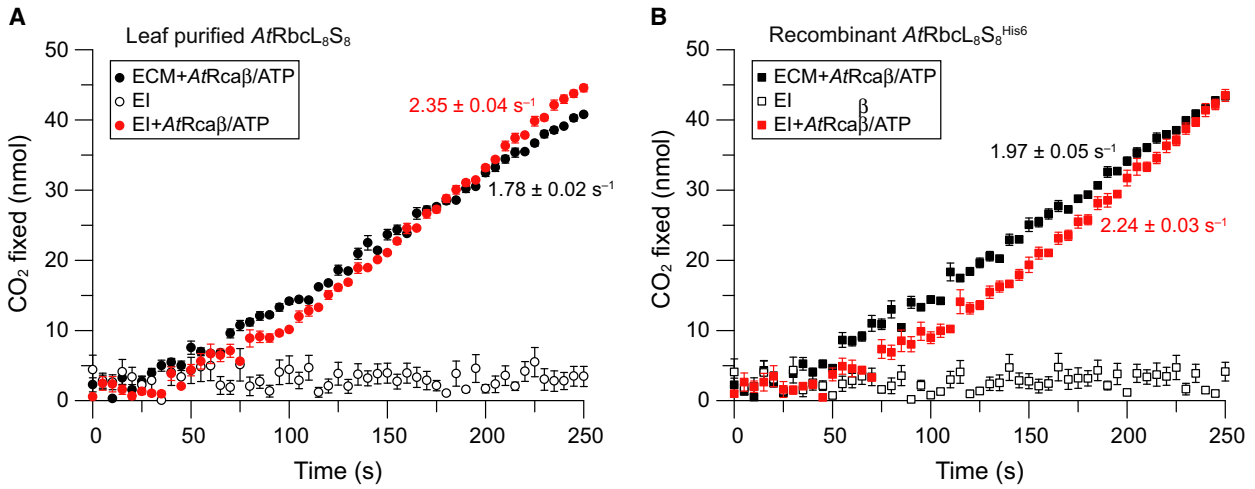

Fig. 6. Reactivation of inhibited *At*RbcL$_8$S$_8$ (A) and *At*RbcL$_8$S$_8^{His6}$ (B) by *Arabidopsis thaliana* Rubisco activase (*At*Rcaβ). RuBP-inhibited Rubisco (EI) was incubated for reactivation with a 10-fold molar excess of *A. thaliana* Rubisco activase (*At*Rcaβ) in the presence ATP (see Materials and methods). Reactivation (red circles and red squares, respectively) was followed by measuring the amount of CO_2 in nmol fixed over time. Carbamylated Rubisco (Rubisco with CO_2 and Mg^{2+}-bound; ECM) (black circles and black squares, respectively) and inhibited Rubisco (EI) (empty circles and empty squares, respectively) were analyzed as controls. The maximum rates of CO_2 fixation for ECM and EI in the presence of *At*Rcaβ and ATP are indicated in $CO_2 \cdot s^{-1}$ per Rubisco active site. The error bars represent SD of $n = 3$ independent experiments.

in variation of copy number and thus fluctuations in expression levels [39]. Thus, applications sensitive to fluctuations of Rubisco expression, such as directed evolution screening [40,41] or metabolic engineering [42–44], may require the use of compatible plasmids.

Acknowledgments

This work was supported by a grant from the Deutsche Forschungsgemeinschaft (DFG) (SFB1035) to MH-H and FUH, and the Minerva foundation of the Max Planck Society (MH-H).

Author contributions

RHW and GT-P performed the experiments. RHW, GT-P, FUH, and MH-H designed the experiments, analyzed the data, and wrote the manuscript.

References

1 Wildner GF (1981) Ribulose-1,5-bisphosphate carboxylase-oxygenase: aspects and prospects. *Physiol Plant* **52**, 385–389.
2 Bracher A, Whitney SM, Hartl FU and Hayer-Hartl M (2017) Biogenesis and metabolic maintenance of Rubisco. *Annu Rev Plant Biol* **68**, 29–60.
3 Erb TJ and Zarzycki J (2018) A short history of RubisCO: the rise and fall (?) of Nature's predominant CO_2 fixing enzyme. *Curr Opin Biotechnol* **49**, 100–107.
4 Hagemann M and Bauwe H (2016) Photorespiration and the potential to improve photosynthesis. *Curr Opin Chem Biol* **35**, 109–116.
5 Aigner H, Wilson RH, Bracher A, Calisse L, Bhat JY, Hartl FU and Hayer-Hartl M (2017) Plant RuBisCo assembly in *E. coli* with five chloroplast chaperones including BSD2. *Science* **358**, 1272–1278.
6 Feiz L, Williams-Carrier R, Wostrikoff K, Belcher S, Barkan A and Stern DB (2012) Ribulose-1,5-bis-phosphate carboxylase/oxygenase accumulation factor1 is required for holoenzyme assembly in maize. *Plant Cell* **24**, 3435–3446.
7 Hauser T, Bhat JY, Milicic G, Wendler P, Hartl FU, Bracher A and Hayer-Hartl M (2015) Structure and mechanism of the Rubisco-assembly chaperone Raf1. *Nat Struct Mol Biol* **22**, 720–728.
8 Feiz L, Williams-Carrier R, Belcher S, Montano M, Barkan A and Stern DB (2014) A protein with an inactive pterin-4a-carbinolamine dehydratase domain is required for Rubisco biogenesis in plants. *Plant J* **80**, 862–869.
9 Wheatley NM, Sundberg CD, Gidaniyan SD, Cascio D and Yeates TO (2014) Structure and identification of a pterin dehydratase-like protein as a Ribulose-bisphosphate carboxylase/oxygenase (RuBisCO) assembly factor in the alpha-carboxysome. *J Biol Chem* **289**, 7973–7981.
10 Fristedt R, Hu C, Wheatley N, Roy LM, Wachter RM, Savage L, Harbinson J, Kramer DM, Merchant SS, Yeates T *et al.* (2018) RAF2 is a RuBisCO assembly factor in *Arabidopsis thaliana*. *Plant J* **94**, 146–156.

11 Brutnell TP, Sawers RJ, Mant A and Langdale JA (1999) Bundle sheath defective2, a novel protein required for post-translational regulation of the rbcL gene of maize. *Plant Cell* **11**, 849–864.
12 Onizuka T, Endo S, Akiyama H, Kanai S, Hirano M, Yokota A, Tanaka S and Miyasaka H (2004) The rbcX gene product promotes the production and assembly of ribulose-1,5-bisphosphate carboxylase/oxygenase of *Synechococcus* sp. PCC7002 in *Escherichia coli*. *Plant Cell Physiol* **45**, 1390–1395.
13 Saschenbrecker S, Bracher A, Rao KV, Rao BV, Hartl FU and Hayer-Hartl M (2007) Structure and function of RbcX, an assembly chaperone for hexadecameric Rubisco. *Cell* **129**, 1189–1200.
14 Liu C, Young AL, Starling-Windhof A, Bracher A, Saschenbrecker S, Rao BV, Rao KV, Berninghausen O, Mielke T, Hartl FU *et al*. (2010) Coupled chaperone action in folding and assembly of hexadecameric Rubisco. *Nature* **463**, 197–202.
15 Bracher A, Starling-Windhof A, Hartl FU and Hayer-Hartl M (2011) Crystal structure of a chaperone-bound assembly intermediate of form I Rubisco. *Nat Struct Mol Biol* **18**, 875–880.
16 Wilson RH and Whitney SM (2017) Improving CO_2 fixation by enhancing Rubisco performance. In Directed Enzyme Evolution: Advances and Applications (Alcalde M, ed.), pp. 101–126, Chapter 4. Springer International Publishing, Cham.
17 Ort DR, Merchant SS, Alric J, Barkan A, Blankenship RE, Bock R, Croce R, Hanson MR, Hibberd JM, Long SP *et al*. (2015) Redesigning photosynthesis to sustainably meet global food and bioenergy demand. *Proc Natl Acad Sci USA* **112**, 8529–8536.
18 South PF, Cavanagh AP, Liu HW and Ort DR (2019) Synthetic glycolate metabolism pathways stimulate crop growth and productivity in the field. *Science* **363**, eaat9077.
19 Parry MA, Andralojc PJ, Scales JC, Salvucci ME, Carmo-Silva AE, Alonso H and Whitney SM (2013) Rubisco activity and regulation as targets for crop improvement. *J Exp Bot* **64**, 717–730.
20 Lin MT and Hanson MR (2018) Red algal Rubisco fails to accumulate in transplastomic tobacco expressing *Griffithsia monilis* RbcL and RbcS genes. *Plant Direct* **2**, e00045.
21 Wilson RH, Alonso H and Whitney SM (2016) Evolving *Methanococcoides burtonii* archaeal Rubisco for improved photosynthesis and plant growth. *Sci Rep* **6**, 22284.
22 Wilson RH and Hayer-Hartl M (2018) Complex chaperone dependence of Rubisco biogenesis. *Biochemistry* **57**, 3210–3216.
23 Baker RT, Catanzariti AM, Karunasekara Y, Soboleva TA, Sharwood R, Whitney S and Board PG (2005) Using deubiquitylating enzymes as research tools. *Methods Enzymol* **398**, 540–554.
24 Kido M, Yamanaka K, Mitani T, Niki H, Ogura T and Hiraga S (1996) RNase E polypeptides lacking a carboxyl-terminal half suppress a mukB mutation in *Escherichia coli*. *J Bacteriol* **178**, 3917–3925.
25 Kubien DS, Brown CM and Kane HJ (2011) Quantifying the amount and activity of Rubisco in leaves. *Methods Mol Biol* **684**, 349–362.
26 Tsai YC, Lapina MC, Bhushan S and Mueller-Cajar O (2015) Identification and characterization of multiple Rubisco activases in chemoautotrophic bacteria. *Nat Commun* **6**, 8883.
27 Lorimer GH and Miziorko HM (1980) Carbamate formation on the epsilon-amino group of a lysyl residue as the basis for the activation of ribulosebisphosphate carboxylase by CO_2 and Mg^{2+}. *Biochemistry* **19**, 5321–5328.
28 Jordan DB and Chollet R (1983) Inhibition of Ribulose bisphosphate carboxylase by substrate ribulose-1,5-bisphosphate. *J Biol Chem* **258**, 13752–13758.
29 Portis AR Jr (2003) Rubisco activase – Rubisco's catalytic chaperone. *Photosynth Res* **75**, 11–27.
30 Bhat JY, Thieulin-Pardo G, Hartl FU and Hayer-Hartl M (2017) Rubisco activases: AAA+ chaperones adapted to enzyme repair. *Front Mol Biosci* **4**, 20.
31 Mueller-Cajar O (2017) The diverse AAA+ machines that repair inhibited Rubisco active sites. *Front Mol Biosci* **4**, 31.
32 Zhang N, Schurmann P and Portis AR Jr (2001) Characterization of the regulatory function of the 46-kDa isoform of Rubisco activase from *Arabidopsis*. *Photosynth Res* **68**, 29–37.
33 Nagarajan R and Gill KS (2018) Evolution of Rubisco activase gene in plants. *Plant Mol Biol* **96**, 69–87.
34 Stotz M, Mueller-Cajar O, Ciniawsky S, Wendler P, Hartl FU, Bracher A and Hayer-Hartl M (2011) Structure of green-type Rubisco activase from tobacco. *Nat Struct Mol Biol* **18**, 1366–1370.
35 Wachter RM, Salvucci ME, Carmo-Silva AE, Barta C, Genkov T and Spreitzer RJ (2013) Activation of interspecies-hybrid Rubisco enzymes to assess different models for the Rubisco-Rubisco activase interaction. *Photosynth Res* **117**, 557–566.
36 Conlan B, Birch R, Kelso C, Holland S, De SA, Long SP, Beck JL and Whitney SM (2018) BSD2 is a Rubisco-specific assembly chaperone, forms intermediary hetero-oligomeric complexes, and is nonlimiting to growth in tobacco. *Plant, Cell Environ* https://doi.org/10.1111/pce.13473
37 Su PH and Li HM (2010) Stromal Hsp70 is important for protein translocation into pea and *Arabidopsis* chloroplasts. *Plant Cell* **22**, 1516–1531.
38 Bölter B and Soll J (2016) Once upon a time – chloroplast protein import research from infancy to future challenges. *Mol Plant* **9**, 798–812.

39 Sathiamoorthy S and Shin JA (2012) Boundaries of the origin of replication: creation of a pET-28a-derived vector with p15A copy control allowing compatible coexistence with pET vectors. *PLoS ONE* **7**, e47259.
40 Wilson RH, Martin-Avila E, Conlan C and Whitney SM (2018) An improved Escherichia coli screen for Rubisco identifies a protein-protein interface that can enhance CO2-fixation kinetics. *J Biol Chem* **293**, 18–27.
41 Engqvist MKM and Rabe KS (2019) Applications of protein engineering and directed evolution in plant research. *Plant Physiol* **179**, 907–917.
42 Schada von Borzyskowski L, Carrillo M, Leupold S, Glatter T, Kiefer P, Weishaupt R, Heinemann M and Erb TJ (2018) An engineered Calvin-Benson-Bassham cycle for carbon dioxide fixation in *Methylobacterium extorquens* AM1. *Metab Eng* **47**, 423–433.
43 Kubis A and Bar-Even A (2019) Synthetic biology approaches for improving photosynthesis. *J Expt Bot erz029*, https://doi.org/10.1093/jxb/erz029
44 Leister D (2019) Genetic engineering, synthetic biology and the light reactions of photosynthesis. *Plant Physiol* **179**, 778–793.

Supporting information

Additional supporting information may be found online in the Supporting Information section at the end of the article.

Fig. S1. Purification of $At\text{RbcL}_8\text{S}_8^{\text{His6}}$ by Ni-NTA affinity chromatography.

Fig. S2. Size-exclusion chromatography of pooled fractions of $At\text{RbcL}_8\text{S}_8^{\text{His6}}$ obtained by Ni-NTA affinity chromatography.

Table S1. List of primers used in this study.